

# Non-singular Terminal Sliding Mode Control for Landing on Asteroids Based on RBF Neural Network

K.P.Liu, F.X.Liu, S.S.Liu and Y.C.Li

**Abstract**—A method of non-singular Terminal sliding mode control was proposed for landing asteroids with uncertainty and strong nonlinearity based on RBF neural network. The dynamics of the detector in the landing environment was analyzed, and the nominal trajectory guidance method based on optimal polynomial was designed, by which the consumption of fuel was suboptimal. Controller was designed using non-singular Terminal sliding mode. The influences caused by unknown disturbance and uncertainty during landing phase was compensated by RBF neural network real-time compensation, which could effectively suppress the influence of external disturbance and weaken the system chattering. Simulation results show that the proposed method was effective.

## INTRODUCTION

COMETS and asteroids exploration is one of the most complex missions in the 21st century. Mankind had carried out several times flew, fly around the probe and returning probe samples mission [1]. Japan's Hayabusa spacecraft successfully returned to Earth and brought the "Itokawa" asteroid samples in 2010 [2]. The Chinese "Chang'e-3" successfully soft landed on the moon on Dec.2, 2013.

Due to the small asteroids gravitational potential energy, the landing is highly susceptible to sun detector perturbations and other disturbances [3]. Scholars at home and abroad had obtained great achievements on the studying about spacecraft landing on small bodies. Cui et al. proposed an autonomous closed-loop control method, using the potential function guidance way to confirm the time, the size and the direction when braking each time [4]. Mei jie et al. proposed a robust adaptive control, making the acceleration difference of gravity to be the interaction, and supposing there is an unknown upper bound, to amend the adaptive control law [5]. A sliding mode variable structure guidance and control system was proposed by Li Shuang et al. divided the control law into equivalent control and compensation control using the equivalent control method [6]. Zhang Guoming et al. achieve the disturbance dynamics of early warning satellites adaptive learning based on the RBF neural

network structural properties, reducing the chattering of the system [7]. Munoz et al. conducted a study on a class of nonlinear discrete robotic arm system, and designed a sliding adaptive controller based on neural networks [8]. Aero-engine system has great time-varying and nonlinear. A sliding mode control method was designed in the paper [9,10], doing the real-time compensation for influences of system disturbances based on neural network characteristics.

The dynamic model of probe is deduced in the landing site coordinate system firstly in this paper. Then the fuel suboptimal guidance law was designed on the basis of full analysis of the probe landing process. Proposed a non-singular Terminal sliding mode control method based on RBF neural network to avoid the singular problem nearby the sliding mode surface and to accelerate reaching at the sliding surface. Using RBF neural network to real time compensate the landing detector with the influences of unknown disturbances and items for no model. The dynamic quality of probe landing control system was improved effectively. The method could satisfy the requirements of flying probe and ensure that the probe landed safely.

## DETECTOR GUIDANCE CONTROL LAW DESIGN

### A. Probe Dynamics Model

The asteroid body-fixed coordinate system  $O_a x_a y_a z_a$ , and the probe landing site coordinate system  $O_l x_l y_l z_l$  are set-up firstly. The  $O_a z_a$  axis coincides with the asteroid's maximum moment of inertia. As probe landing site coordinate system with the origin coinciding with the landing site,  $O_l z_l$  axis for the extension of center of mass and the landing site of attachment.  $\theta$ ,  $\phi$  stand for the longitude and latitude of the landing site location;  $R$  denotes the position vector from the target small body mass center to the probe, as shown in Fig. 1.

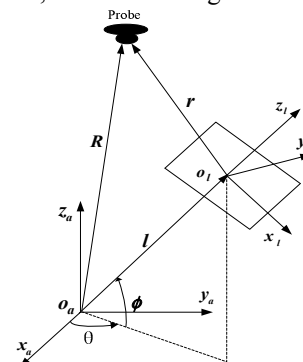


Fig.1. Coordinate systems definition

K. P. Liu is a professor of College of Electrical and Electronic Engineering, Changchun University of Technology, Changchun, CO 130012, China. (e-mail: liukeping@mail.ccut.edu.cn)

F. X. Liu is a master of College of Electrical and Electronic Engineering, Changchun University of Technology, Changchun, CO 130012, China. (e-mail:630673732@qq.com)

S. S. Liu is a professor of College of Electrical and Electronic Engineering, Changchun University of Technology, Changchun, CO 130012, China.(corresponding author. phone: 0431-85716441, fax: 0431-85716441; e-mail: liu-shuaishi@126.com)

Y. C. Li is the director of College of Electrical and Electronic Engineering, Changchun University of Technology, Changchun, CO 130012 China. (e-mail address: liyc@mail.ccut.edu.cn)

This work was supported in part by National Basic Research Program of China (No.2012CB720000)

The dynamic equations of motion for probe in the fixed-body coordinate system are given as follows [11].

$$\ddot{\mathbf{R}}+2\boldsymbol{\omega}\times\dot{\mathbf{R}}+\boldsymbol{\omega}\times(\boldsymbol{\omega}\times\mathbf{R})+\dot{\boldsymbol{\omega}}\times\mathbf{R}=\mathbf{F}+\mathbf{U}+\boldsymbol{\delta} \quad (1)$$

Where  $\mathbf{R}$  denotes the position vector from the mass center of the target asteroid to the probe;  $\boldsymbol{\omega}$  is the angular vector of the asteroid rotation;  $\mathbf{F}$  is the control acceleration;  $\mathbf{U}$  is the gradient of the gravitational potential;  $\boldsymbol{\delta}$  is the perturbative acceleration for no model (including the solar radiation pressure and third-body gravitational perturbations).

Assuming that the asteroid at a fixed angular velocity  $\omega_a$  around the  $z$  axis of rotation, we can define  $\boldsymbol{\omega}\equiv\boldsymbol{\omega}_a=[0 \ 0 \ \omega_a]^T$ , then  $\dot{\boldsymbol{\omega}}=0$ , the expression of dynamic model in the landing point coordinates is

$$\begin{aligned} \ddot{x}-2\omega_a\sin\phi\dot{y}-\omega_a^2\sin^2\phi x-\omega_a^2\sin\phi\cos\phi z &=F_x+U_x+\delta_x \\ \ddot{y}+2\omega_a\sin\phi\dot{x}+2\omega_a\cos\phi\dot{z}-\omega_a^2y &=F_y+U_y+\delta_y \\ \ddot{z}-2\omega_a\cos\phi\dot{y}-\omega_a^2\sin\phi\cos\phi x-\omega_a^2\cos^2\phi z &=F_z+U_z+\delta_z \end{aligned} \quad (2)$$

Where  $\theta$ ,  $\phi$  is the longitude and latitude of the landing site location;  $F_x$ ,  $F_y$ ,  $F_z$  are components of control acceleration;  $U_x$ ,  $U_y$ ,  $U_z$  are components of the asteroid gravitational potential [12].

## B. Detector Guidance Control Law Design

### 1) Nominal Trajectory Guidance Law

To ensure the detector complete the speed adjustment and attitude adjustment under the limited thrust, planning the trajectory equation for the detector to satisfy boundary conditions based on the fuel optimal guidance theory.

$$r_z(t)=a_0+a_1t+a_2t^2+a_3t^3 \quad (3)$$

Assuming the landing time is  $\tau$ , the boundary condition is given by

$$\left. \begin{aligned} r_z(0) &= z_0 \\ r_z(\tau) &= z_n \\ \dot{r}_z(0) &= \dot{z}_0 \\ \dot{r}_z(\tau) &= 0 \end{aligned} \right\} \quad (4)$$

Where  $z_0$  denotes the initial position of the probe,  $z_n$  denotes the probe's terminal location,  $\dot{z}_0$  denotes the initial high rate of change. According to the initial and terminal position and velocity of the detector, we can get the parameter values in  $r_z(t)$ . The cubic curve to satisfy the boundary condition and the planned descent velocity is given as follow:

$$r_z(t)=z_0+\dot{z}_0t+(3z_n-3z_0-2\dot{z}_0\tau)\frac{t^2}{\tau^2}+(2z_0+\dot{z}_0\tau-2z_n)\frac{t^3}{\tau^3} \quad (5)$$

$$\dot{r}_z(t)=\dot{z}_0+(6z_n-6z_0-4\dot{z}_0\tau)\frac{t}{\tau^2}+(6z_0+3\dot{z}_0\tau-6z_n)\frac{t^2}{\tau^3} \quad (6)$$

By this way, the velocity trajectory of x-axis and y-axis

are also planned.

### 2) RBF Neural Network Sliding Mode Controller Design.

Define the tracking error and the velocity tracking error as  $e=r-r_d$  and  $\dot{e}=\dot{r}-\dot{r}_d$ , where  $r_d=[r_x, r_y, r_z]^T$  denotes the reference trajectory.

If  $[e_1 \ e_2 \ e_3 \ e_4 \ e_5 \ e_6]=[x-r_x \ y-r_y \ z-r_z \ \dot{x}-\dot{r}_x \ \dot{y}-\dot{r}_y \ \dot{z}-\dot{r}_z]$ , then the Eq.(2) can be converted into the type:

$$\begin{bmatrix} \dot{e}_1 \\ \dot{e}_2 \\ \dot{e}_3 \end{bmatrix} = \begin{bmatrix} e_4 \\ e_5 \\ e_6 \end{bmatrix} \quad (7)$$

$$\begin{bmatrix} \dot{e}_4 \\ \dot{e}_5 \\ \dot{e}_6 \end{bmatrix} = \begin{bmatrix} -\ddot{r}_x+2\omega_a\sin\phi\dot{y}+F_x+U_x+\delta_x \\ -\ddot{r}_y-2\omega_a\sin\phi\dot{x}-2\omega_a\cos\phi\dot{z}+F_y+U_y+\delta_y \\ -\ddot{r}_z+2\omega_a\cos\phi\dot{y}+F_z+U_z+\delta_z \end{bmatrix} \quad (8)$$

Eq.(7) and Eq.(8) could be transformed into state equations

$$\begin{cases} \dot{e}_i = e_j \\ \dot{e}_j = f_k + g_k + u_k \end{cases} \quad (9)$$

Where  $e_i$  and  $e_j$  ( $i=1,2,3; j=4,5,6$ ) denote the system state variables,  $f_k$  denotes nonlinearities of the system,  $g_k$  denotes uncertainties and disturbances and it is satisfied with  $\|\bar{g}_k\|\leq l_g, l_g > 0$ ,  $u_k$  denotes control law ( $k=x, y, z$ ).

$$\begin{aligned} f_k &= \begin{bmatrix} -\ddot{r}_x+2\omega_a\sin\phi\dot{y}+U_x \\ -\ddot{r}_y-2\omega_a\sin\phi\dot{x}-2\omega_a\cos\phi\dot{z}+U_y \\ -\ddot{r}_z+2\omega_a\cos\phi\dot{y}+U_z \end{bmatrix} \\ g_k &= [\delta_x \ \delta_y \ \delta_z]^T, \quad u_k = [F_x \ F_y \ F_z]^T. \end{aligned}$$

The non-singular Terminal sliding mode based on exponential approach law can avoid the singular problem nearby the sliding mode surface. Improve the speed of approaching the sliding surface and reduce the adjustment time of the controller. Ensure the detector response rapidly and stability during the landing phase.

So, select detector non-singular Terminal sliding mode surface as follow:

$$s_i = e_i + \frac{1}{\beta}(e_j)^{p/q} \quad (10)$$

Where  $\beta > 0$ ,  $p/q \in (1, 2)$ . The Eq.(10) can be proved to have no negative powers, so as to avoid the singular problem [13].

In order to keep the control law responds immediately, we use the exponential reaching law to approach the sliding surface  $\dot{s} = -\varepsilon \operatorname{sgn}(s) - ks, \varepsilon > 0, k > 0$ , and taking the first-order derivative of  $s_i$ .

$$\dot{s}_i = \dot{e}_i + \frac{1}{\beta} \frac{p}{q} (e_j)^{p/q-1} \dot{e}_j = \dot{e}_j + \frac{1}{\beta} \frac{p}{q} (e_j)^{p/q-1} (\mathbf{f}_k + \mathbf{g}_k + \mathbf{u}_k) \quad (11)$$

Suppose  $\rho(e_j) = \frac{1}{\beta} \frac{p}{q} (e_j)^{p/q-1}$ , get the control law  $\mathbf{u}_k$ .

$$\mathbf{u}_k = -\rho^{-1}(e_j)[\dot{e}_j + \rho(e_j)(\mathbf{f}_k + \mathbf{g}_k) + \varepsilon \operatorname{sgn}(s_i) + ks_i] \quad (12)$$

When taking no consideration of the disturbance influences to the system and neglecting  $\mathbf{g}_k$ , we will get the equivalent control law:

$$\mathbf{u}_{eq} = -\beta \frac{q}{p} (e_j)^{2-p/q} - \mathbf{f}_k - ks_i - (l_g + \varepsilon) \operatorname{sgn}(s_i) \quad (13)$$

RBF neural network is a kind of forward with three layers and has faster learning rate. Its structure diagram is as shown in Fig.2.

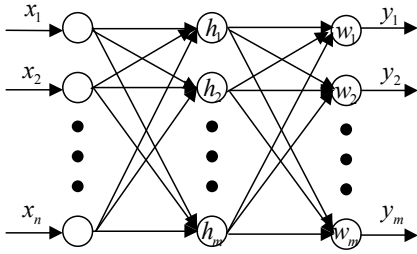


Fig.2. RBF network structure diagram

Here  $\mathbf{X} = [x_1 \ x_2 \ \dots \ x_n]^T$  is the input vector of the RBF network structure. Suppose the radial basis vector is  $\mathbf{H} = [h_1 \ h_2 \ \dots \ h_m]^T$ ,  $h_j$  is Gaussian function,  $\mathbf{B} = [b_1 \ b_2 \ \dots \ b_m]^T$  is the base width vector,  $\mathbf{W} = [w_1 \ w_2 \ \dots \ w_m]^T$  is the weight vector.

$$h_j = \exp\left(-\frac{\|\mathbf{X} - \mathbf{c}_j\|^2}{2b_j^2}\right) \quad (14)$$

$$\mathbf{c}_j = [c_1 \ c_2 \ \dots \ c_m] \quad j = 1, 2, \dots, m.$$

Choosing  $\mathbf{e}_i, \mathbf{e}_j$  as the input of the neural network, and equivalent compensation control  $\mathbf{u}_n = \mathbf{W}^T \mathbf{H}$  as the output. Then the system control law can be expressed as  $\mathbf{u}_k = \mathbf{u}_{eq} + \mathbf{u}_n$ .

The difference of the neural network output and the actual output of the system is  $\Delta u_{kn} = [\Delta u_1 \ \Delta u_2 \ \dots \ \Delta u_n]$ . We choose  $Q = \frac{1}{2} (\Delta u_n)^2$  as the networks' learning indicator.

Based on the gradient-descent method, the weight learning algorithm of the neural network can be gained as follows:

$$\Delta w_j = -\eta \frac{\partial Q}{\partial w_j} = -\eta \Delta u_n \frac{\partial \Delta u_n}{\partial w_j} = -\eta \Delta u_n h_j$$

$$w_j(k) = w_j(k-1) + \Delta w_j + \alpha [w_j(k-1) - w_j(k-2)]$$

$$\Delta b_j = -\eta \frac{\partial Q}{\partial b_j} = -\eta \Delta u_n \frac{\partial \Delta u_n}{\partial b_j} = -\eta \Delta u_n w_j h_j \frac{\|\mathbf{x}_n - \mathbf{c}_j\|^2}{b_j^3}$$

$$b_j(k) = b_j(k-1) + \Delta b_j + \alpha [b_j(k-1) - b_j(k-2)]$$

$$\Delta c_{ji} = -\eta \frac{\partial Q}{\partial c_j} = -\eta \Delta u_n \frac{\partial \Delta u_n}{\partial c_j} = -\eta \Delta u_n w_j \frac{x_{nj} - c_{ji}}{b_j^2}$$

$$c_{ji}(k) = c_{ji}(k-1) + \Delta c_{ji} + \alpha [c_{ji}(k-1) - c_{ji}(k-2)]$$

Where  $\eta$  denotes the learning rate,  $\alpha$  denotes the inertia coefficient,  $i$  denotes the number of input layers,  $j$  denotes the number of hidden layers.

### C. Stability Proof

Selecting Lyapunov function as follows:

$$V = V_1 + V_2 \quad (15)$$

$$V_1 = \frac{1}{2} s_i^2, \quad V_2 = \frac{1}{2} M^2 = \frac{1}{2} Q$$

$$\dot{V}_1 = s_i \dot{s}_i = -s_i \rho(e_j) [\varepsilon \operatorname{sgn}(s_i) + ks_i + l_g \operatorname{sgn}(s_i)] \quad (16)$$

$$\leq -s_i (\varepsilon \operatorname{sgn}(s_i) + ks_i) < 0$$

Command

$$\Delta V_2(k) = V_2(k+1) - V_2(k) = \frac{1}{2} [M^2(k+1) - M^2(k)]$$

Where

$$M(k+1) = M(k) + \Delta M(k) \quad (17)$$

$$\Delta M(k) = \frac{\partial M(k)}{\partial w_j} \Delta w_j \quad (18)$$

$$\Delta w_j = -\eta \frac{\partial Q}{\partial w_j} = -\eta \frac{\partial [M^2(k)]}{\partial w_j} \quad (19)$$

$$= -2\eta M(k) \frac{\partial [M(k)]}{\partial w_j}$$

Taking Eq.(19)~(21) into  $\Delta V_2(k)$ , then

$$\Delta V_2(k) = \frac{1}{2} \{ [M(k) + \Delta M(k)]^2 - M^2(k) \} = \frac{1}{2} [2M(k)\Delta M(k) + \Delta M^2(k)]$$

$$= \frac{1}{2} \{ -4\eta M^2(k) \left[ \frac{\partial [M(k)]}{\partial w_j} \right]^2 + 4\eta^2 M^2(k) \left[ \frac{\partial [M(k)]}{\partial w_j} \right]^2 \}$$

$$= 2M^2(k) \left[ \frac{\partial [M(k)]}{\partial w_j} \right]^2 (\eta^2 - \eta)$$

When taking  $0 < \eta < 1$ , we can get  $\Delta V_2(k) < 0$ , so  $\dot{V} < 0$ .

The tracking control law is proved to be stable.

SIMULATION AND ANALYSIS

Taking one asteroid as the target small body, and its parameters are listed in Table 1(Zhang Z.X et al. 2012; Li S et al. 2006).

TABLE 1  
NUMERICAL SIMULATION PARAMETERS

Parameters	Real value	Simulation parameters
$u_a$	4.749E-04	4.800E-04
Spin period (h)	10.54	10.55
$R_\theta$ (km)	1.150	1.148
$C_{20}$	-0.113	-0.110
$C_{22}$	0.0396	0.0397
$C_{40}$	0.068	0.069
$C_{42}$	0.0032	0.0031
$C_{44}$	2.790E-04	2.780E-04
$K_{Px} = K_{Py} = K_{Pz}$		0.0005
$K_{Dx} = K_{Dy} = K_{Dz}$		0.05
Descending position		[3550,4050,11000]
Descending velocity		[-2.2,1.2,-9]
Landing position		[300,300,2000]
Landing velocity		[-1.2,0.2,-1]
Landing final site		[20,20,20]

Choose the parameters of non-singular Terminal sliding mode control:  $\beta=2$ ,  $p/q=1.5$ ,  $k=2$ ,  $l_g=0.015$ . The x, y, z-axis position and velocity are designed as RBF network input. By using three groups of the 2-6-1 network structure, we select  $W=[0.1 \ 0.1 \ 0.1 \ 0.1 \ 0.1 \ 0.1]^T$  as the initial value of network weights,  $B=[0.1 \ 0.1 \ 0.1 \ 0.1 \ 0.1 \ 0.1]^T$  as the base width vector,  $c = \begin{bmatrix} 0.1 & 0.1 & 0.1 & 0.1 & 0.1 & 0.1 \\ 0.1 & 0.1 & 0.1 & 0.1 & 0.1 & 0.1 \end{bmatrix}$  as the nodal center vector,  $\eta=0.6$  as the learning rate,  $\alpha=0.05$  as the inertial coefficient. In the landing phase, the simulation results are shown in Fig.3. to Fig.7.

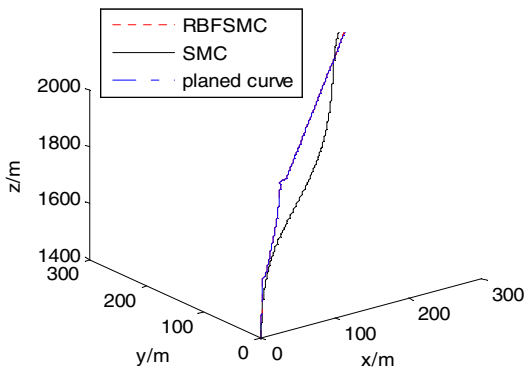


Fig.3. Landing trajectory based on RBF sliding mode

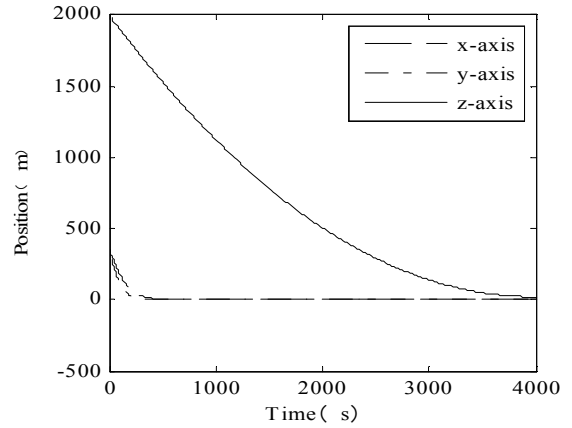


Fig.4. Curve of landing phase position

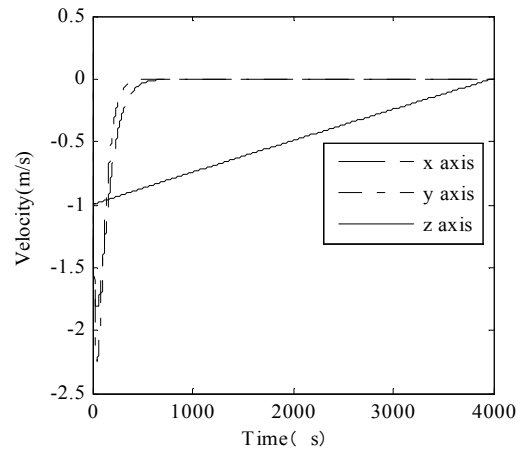


Fig.5. Curve of landing phase velocity

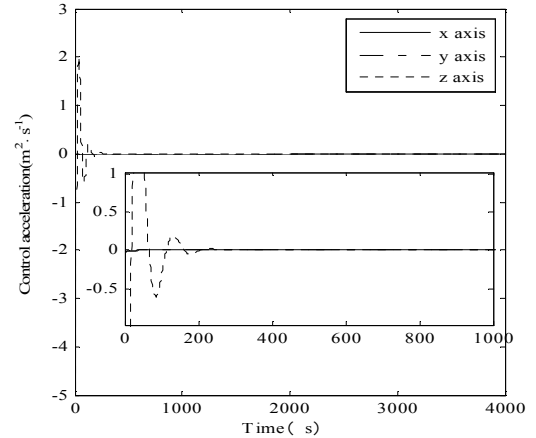


Fig.6. Curve of control acceleration

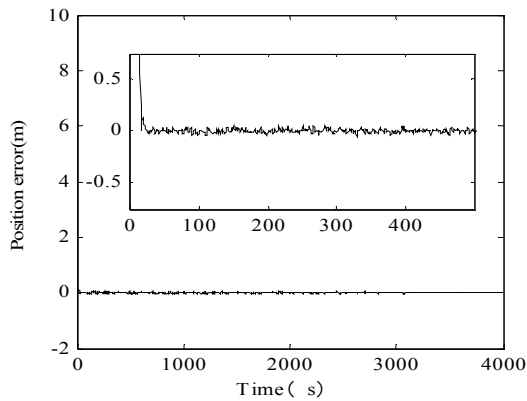


Fig.7. Curve of landing phase position error with RBFSMC controller

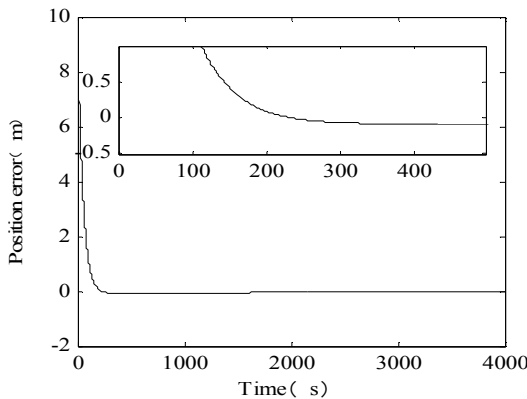


Fig.8 Curve of landing phase position error with SMC controller

Fig.3 gives the probe's three dimensional landing trajectory curve based on the non-singular Terminal sliding mode control with the compensation control of RBF network. Compared with the general sliding mode control the detector based on the non-singular Terminal sliding mode control is stable operation and has small chattering. It also can follow the tracks of nominal trajectory accurately. The probe turns to be vertical landing when at height of 1400 meters in the z axis. Fig.4 to Fig.6 show the position, velocity and control acceleration time history of the probe, the control force can be satisfied with engineering requirements. Fig.7 and Fig.8 show the distinction of the detector position error of z-axis in the landing phase for the RBF neural network real-time compensation control and the traditional sliding mode control. From the curves we can clearly see that under the control of RBF neural network real-time compensation, the convergence rate of trajectory error is significantly faster than that of traditional sliding mode. Control convergence time is shorter and control effect is well.

## CONCLUSION

In this paper, a method of non-singular Terminal sliding mode control was proposed for landing probe with uncertainty and nonlinearity based on RBF neural network. The controller could avoid the singular problem nearby the sliding mode surface and ensure the probe accelerate

reaching at the siding surface. Using RBF neural network to real time compensate the landing probe with the influences of unknown disturbances and items for no model. Research results show that the controller designed in this paper has good effect in reducing the chattering of the system, and could make sure the probe vertically land on the scheduled landing site. Ensure that the probe landing safely and accurately finally.

## REFERENCES

- [1] Rayman M.D., Fraschetti T.C., and Raymond C.A. et al. "A Mission in development for exploration of main belt asteroid Vesta and Ceres," *Acta Astronautica*, 2006, 58(11):605-616.
- [2] Kuninaka H, and Kawaguchi J. "Lessons learned form round trip of Hayabusa asteroid explorer in deep space," *IEEE Aerospace Conference*, 2011:1-8.
- [3] Lara, M. and Scheeres, D. J. "Stability bounds for three-dimensional motion close to asteroids," *Journal of the Astronautical Sciences*, 2002, Vol 50(4):389-409.
- [4] P.Y.Cui, S.Y.Zhu, and H.T.Cui. "Research on maneuvering control of small objects autonomous soft landing," *Acta Astronautica*, 2008 29(2):121-126.
- [5] J.Mei and G.F.Ma, "Robust adaptive control based on relative orbit of the closing probe," *Acta Astronautica*, 2010,31(10) :2276-2282.
- [6] S.Li and P.Y.Cui., "Variable structure with sliding mode control for landing on asteroids" *Acta Astronautica*, 2005, 26(6) :808-812.
- [7] M.G.Zhang, Y.H.Geng, and L.H.Jia, "Based on RBF network upper bound of the adaptive learning early warning satellite sliding mode control," *Journal of Jilin university (engineering science)*, 2007,37(4):959-964.
- [8] Munoz D and Sbarbaro D, "An adaptive sliding-mode controller for discrete nonlinear systems," *IEEE Transactions on Industrial Electronics*, 2002, 47(3): 574-581.
- [9] Z.G.Miao, S.S.Xie, H.T.Wang, X.S.Zhai, Z.Y.Zhang, and X.D.Sun, "Terminal sliding mode controller for aero-engine base on RBF neural network," *Journal of Aerospace Power*, 2010,25(12):2281-2286.
- [10] Y.Li and D.Fan, "Fuzzy sliding mode controller for aero-engine based on RBF neural network," *Computer Measurement & Control*, 2013,21(3):632-634.
- [11] Z.X,et al. "Robust sliding mode guidance and control for soft landing on small bodies," *Journal of the Franklin Institute* 349 (2012) 493-509.
- [12] Washabaugh P.D.and Scheeres D.J., "Energy and stress distributions in ellipsoids," *Icarus*, 2002 , 159(2) :314-321.
- [13] Y.Feng, X.Yu, and Z.Man, "Non-singular terminal sliding mode control of rigid manipulators," *Automatica*, 2002, 38(12): 2159-2167.